Medicinal Chemistry Research (2023) 32:85–98
https://doi.org/10.1007/s00044-022-02993-w

MEDICINAL CHEMISTRY RESEARCH

ORIGINAL RESEARCH

Synthesis, antimicrobial, and antioxidant activities of disubstituted 1,2,3-triazoles with amide-hydroxyl functionality

Manisha Chahal[1] · Chander Prakash Kaushik[1] · Raj Luxmi[1] · Devinder Kumar[1] · Ashwani Kumar[1]

Received: 21 August 2022 / Accepted: 4 November 2022 / Published online: 17 November 2022

Abstract

A series of 1,4-disubstituted 1,2,3-triazoles with amide-hydroxyl functionality **(5a–5t)** was synthesized from aliphatic alkynes **(4a–4e)** and aromatic bromides **(3a–3d)** in presence of catalytic amount of cellulose CuI nanoparticles. All the synthesized triazoles were characterized by various analytical techniques: FTIR, ^{1}H NMR, ^{13}C NMR and HRMS. Further, all the synthesized compounds were screened for in vitro antioxidant and antimicrobial activities. The antioxidant activity of the compound **5s** was found better than other compounds. Compounds **5h** and **5l** exhibited good antibacterial and antifungal activity, respectively. The docking studies were performed to find out various binding interactions of protein-ligand complex. In silico ADME study was performed to evaluate their drug likeness.

Keywords 1,4-disubstituted 1,2,3-triazoles · Cell-CuI NPs · Antioxidant activity · Antimicrobial activity

Introduction

The day-by-day increase of infectious diseases due to multi-drug resistance, which often results from the over-expression of multi-drug efflux systems and their wide-spread usage has hampered the effective treatment of different human diseases caused by various microbes [1, 2]. These circumstances stimulate an essential need for integral efforts to synthesize new classes of antimicrobial agents, particularly, structurally diverse molecules with unique mechanism of action, high potency, less toxicity, and no or fewer side effects [3].

On the other hand, many chemotherapeutic agents act by producing free radicals and causing oxidative stress in normal cells. The oxidative stress reflects an imbalance between the oxidants and the antioxidants and believed to be associated with multiple diseases such as inflammation, cancer, myocardial infraction, arthritis and neurodegenerative disorders, mutagenesis, genotoxicity [4]. Antioxidants can minimize or inhibit oxidative damage by regulating the generation and elimination of reactive oxygen species (ROS) like hydroxyl and superoxide radicals. Therefore, the development of novel antioxidants attained great importance in organic chemistry.

In this context, the nitrogen heterocyclic pharmacophores, 1,2,3-triazoles occupy protuberant place [5] in medicinal chemistry owing to unique structural features with multifarious pharmaceutical activities. As triazole is the bioisostere of amide and capable of forming hydrogen-bonding which in turn improves their solubility and ability to interact with biomolecular targets [6]. Moreover, they are stable under acidic as well as basic hydrolysis, and also oxidative and reductive stresses due to their high aromatic stabilization [7]. Literature studies revealed that 1,2,3-triazoles exhibit a wide range of biological applications indicating that this moiety is a template potentially useful in medicinal chemistry research and therapeutic applications like antimicrobial [8–12], anticonvulsant [13], antitubercular [14–16], antidiabetic [17], antimalarial [18, 19], antioxidant [20–22], anticancer [23–25], anti-inflammatory [26], antileishmanial [27], antiviral [28], anti-hypertensive [29], acetylcholinesterase inhibitory [30] and O-GlcNAcase (OGA) inhibitory [31] activities etc. Several 1,2,3-triazole-containing drug molecules including tazobactum, carboxyamidotriazole are also available in the market.

Several methods have been employed for the synthesis of 1,2,3-triazoles [32, 33]. Huisgen gave 1,3-dipolar

Supplementary information The online version contains supplementary material available at https://doi.org/10.1007/s00044-022-02993-w.

✉ Chander Prakash Kaushik
kaushikcp@gmail.com

[1] Department of Chemistry, Guru Jambheshwar University of Science & Technology, Hisar, Haryana, India

cycloaddition reaction between terminal alkyne and azide for making triazole ring [34, 35]. Fokin and Sharpless in 2002 introduced a method for regioselective synthesis of 1,4-disubstituted 1,2,3-triazoles in the presence of copper(I) catalyst [36].

Keeping in view and continuation of our previous studies of amide-linked 1,4-disubstituted 1,2,3-triazoles [37] with good pharmacological properties, here, we described the synthesis of a series of triazole scaffolds having amide and hydroxyl linkage using cellulose supported CuI nanoparticles and investigated for antimicrobial and antioxidant activities with docking and ADME studies.

Result and discussion

Chemistry

The synthetic pathways adopted for the synthesis of amide and hydroxyl functionality containing 1,4-disubstituted 1,2,3-triazoles **(5a-5t)** have been presented in Scheme 2a, 2b, and 2c.

Synthesis of 4-(bromomethyl)-N-arylbenzamides **(3a-3d)** [Scheme 1] was carried out from the reaction of 4-(bromomethyl)benzoylbromide **(1)** with different aniline derivatives **(2a-2d)** using potassium carbonate in dichloromethane. The commercially available terminal alkynes, prop-2-yn-1-ol **(4a)**, 2-methylbut-3-yn-2-ol **(4b)**, 3-methylpent-1-yn-3-ol **(4c)**, but-3-yn-1-ol **(4d)** and pent-4-yn-1-ol **(4e)** were used in synthesis. Then 4-(bromomethyl)-N-arylbenzamides **(3a-3d)**, was treated with sodium azide and terminal alkynes **(4a-4e)** in presence of Cell-CuI NPs in water at 60–70 °C for 6–10 h to afford 1,4-disubstituted 1,2,3-triazoles with amide and hydroxyl functionality **(5a-5t)** in good yield [Scheme 2a, Scheme 2b, Scheme 2c].

Structure elucidation of synthesized 1,4-disubstituted 1,2,3-triazoles **(5a–5t)** was carried out through FTIR, ^{1}H, ^{13}C NMR & HRMS. The FTIR spectra of the synthesized triazoles showed characteristic absorption band in region 3477–3334 cm^{-1} and 3350–3261 cm^{-1} due to O-H and N-H stretching vibration of amide, respectively while band in the region 3149–3112 cm^{-1} and 1683–1646 cm^{-1} were assigned to C–H stretching of triazole ring and C=O stretching of amide group, respectively. The ^{1}H NMR spectra of all the compounds displayed two characteristic singlets in the region δ 10.18–10.89 and δ 7.83–8.08 due to N-H and triazolyl proton, respectively. A singlet due to methylene protons attached to N_1 of triazole appeared in the region δ 5.20–5.69. Moreover, in ^{13}C NMR spectra a characteristic signal of carbonyl carbon appeared in range δ 165.2–166.6 whereas C_4 and C_5 of triazole ring resonated in region δ 147.3–148.9 and δ 119.9–122.6, respectively. Carbon attached to OH group showed a signal in the range δ 55.5–70.3 and methylene carbon attached to N_1 of the triazole ring appeared in region δ 52.8–56.3. Further, the results obtained from high-resolution mass spectrometry (HRMS) were found in accordance with theoretically predicted molecular masses.

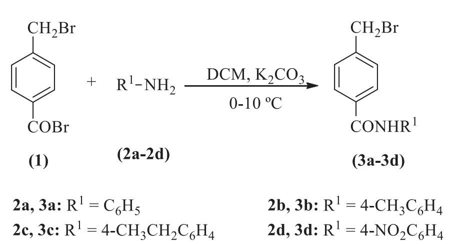

Scheme 1 Synthesis of 4-(bromomethyl)-N-arylbenzamides

Antimicrobial activities

Antibacterial activity

All the synthesized 1,4-disubstituted 1,2,3-triazoles were screened for antibacterial activity against *S. gordonii (MTCC 2695), B. subtilis (MTCC 441), E. coli (MTCC1231)*, and K. pneumoniae *(NCDC 138)* via serial dilution method. Results were compared with the standard drug Ciprofloxacin in term of minimum inhibitory concentration (MIC, μmol/mL; Table 1). The synthesized 1,2,3-triazoles showed moderate to good antibacterial activity. Compounds **5e, 5f, 5g**, and **5h** (MIC = 0.038, 0.036, 0.035, and 0.033 μmol/mL, respectively) showed good antibacterial activity against *S. gordonii* and *B. subtilis* strains. In case of *K. pneumoniae*, compounds **5b** and **5e** (MIC = 0.039, 0.038 μmol/mL, respectively) displayed good activity while compounds **5e, 5f, 5g, 5h**, and **5k** (MIC = 0.038, 0.036, 0.035, 0.033 and 0.033 μmol/mL respectively) showed appreciable activity against *E. coli.*

Following Structure–Activity Relationship has been drawn from above data:—

1. In most of the cases, substitution on phenyl ring attached to nitrogen of amide group leads to improved antibacterial activity compared to unsubstituted counterpart.
2. Triazoles having nitro group on phenyl ring showed enhanced activity than methyl/ethyl substituted congeners in most of the cases.
3. Generally, ethyl group on phenyl ring favored antibacterial activity compared to methyl-substituted congeners.
4. It has been observed that presence of alkyl group on carbon attached to OH group improved antibacterial activity.
5. Generally, triazoles with larger carbon chain present at C_4 of triazole ring showed improved antibacterial activity.

a

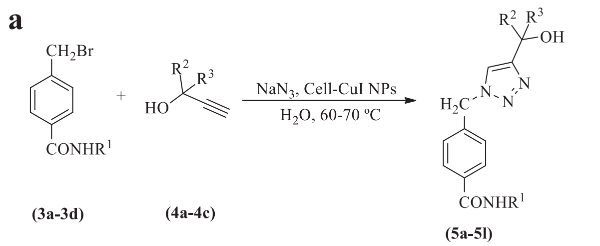

4a: $R^2 = H$, $R^3 = H$ **4b**: $R^2 = CH_3$, $R^3 = CH_3$
4c: $R^2 = CH_3$, $R^3 = CH_2CH_3$

Compounds	R^1	R^2	R^3
5a	C_6H_5	H	H
5b	4-$CH_3C_6H_4$	H	H
5c	4-$CH_3CH_2C_6H_4$	H	H
5d	4-$NO_2C_6H_4$	H	H
5e	C_6H_5	CH_3	CH_3
5f	4-$CH_3C_6H_4$	CH_3	CH_3
5g	4-$CH_3CH_2C_6H_4$	CH_3	CH_3
5h	4-$NO_2C_6H_4$	CH_3	CH_3
5i	C_6H_5	CH_3	C_2H_5
5j	4-$CH_3C_6H_4$	CH_3	C_2H_5
5k	4-$CH_3CH_2C_6H_4$	CH_3	C_2H_5
5l	4-$NO_2C_6H_4$	CH_3	C_2H_5

b

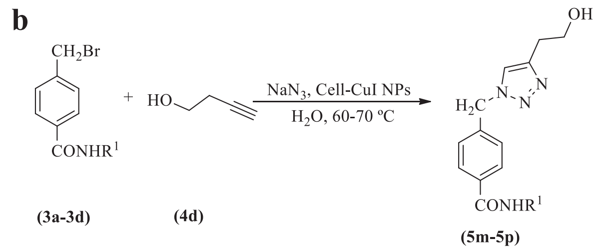

Compounds	R^1	Compounds	R^1
5m	C_6H_5	**5o**	4-$CH_3CH_2C_6H_4$
5n	4-$CH_3C_6H_4$	**5p**	4-$NO_2C_6H_4$

c

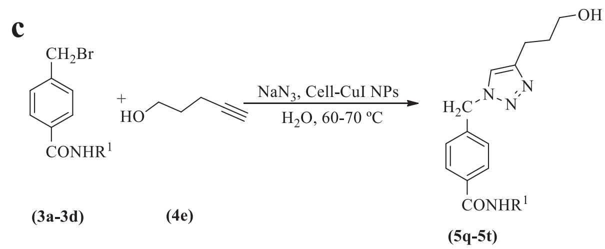

Compounds	R^1	Compounds	R^1
5q	C_6H_5	**5s**	4-$CH_3CH_2C_6H_4$
5r	4-$CH_3C_6H_4$	**5t**	4-$NO_2C_6H_4$

Scheme 2 a-c Synthesis of 1,4-disubstituted 1,2,3-triazoles with amide and hydroxyl functionality.

Table 1 Antibacterial activity of synthesized 1,4-disubstituted 1,2,3-triazoles (**5a–5t**)

Compounds	Minimum Inhibitory concentration (MIC in µmol/mL)			
	Streptococcus gordonii	*Bacillus subtilis*	*Klebsiella pneumoniae*	*Escherichia coli*
5a	0.081	0.081	0.081	0.081
5b	0.078	0.078	0.039	0.078
5c	0.074	0.074	0.149	0.074
5d	0.071	0.071	0.283	0.071
5e	0.038	0.038	0.038	0.038
5f	0.036	0.036	0.071	0.036
5g	0.035	0.035	0.069	0.035
5h	0.033	0.033	0.066	0.033
5i	0.071	0.071	0.071	0.071
5j	0.069	0.069	0.275	0.069
5k	0.066	0.066	0.066	0.033
5l	0.063	0.063	0.126	0.063
5m	0.078	0.078	0.078	0.078
5n	0.074	0.074	0.074	0.074
5o	0.071	0.071	0.143	0.071
5p	0.068	0.068	0.272	0.068
5q	0.074	0.149	0.074	0.074
5r	0.071	0.071	0.071	0.071
5s	0.069	0.069	0.069	0.069
5t	0.066	0.066	0.066	0.066
Ciprofloxacin	0.019	0.019	0.019	0.019

Table 2 Antifungal activity of synthesized 1,4-disubstituted 1,2,3-triazoles (5a–5t)

Compounds	Minimum Inhibitory concentration (MIC in μmol/mL)	
	Candida albicans	*Rhizopus oryzae*
5a	0.041	0.081
5b	0.039	0.078
5c	0.074	0.149
5d	0.035	0.071
5e	0.037	0.074
5f	0.036	0.071
5g	0.034	0.069
5h	0.033	0.066
5i	0.036	0.071
5j	0.034	0.069
5k	0.033	0.066
5l	0.032	0.063
5m	0.039	0.078
5n	0.037	0.074
5o	0.036	0.071
5p	0.034	0.068
5q	0.037	0.074
5r	0.036	0.071
5s	0.034	0.069
5t	0.033	0.066
Fluconazole	0.020	0.020

Antifungal activity

All the synthesized 1,2,3-triazoles were screened for antifungal activity against *Candida albicans* and *Rhizopus oryzae* using serial dilution method. Results were compared with the standard drug Fluconazole in term of minimum inhibitory concentration (MIC, μmol/mL; Table 2).

Compounds **5h, 5k**, 5**l**, and **5t** (MIC = 0.033, 0.033, 0.032, and 0.033 μmol/mL, respectively) showed good activity against fungal strain, *C. albican*. In case of *R. oryzae*, compounds 5**h, 5k, 5l**, and 5**t** (MIC = 0.066, 0.066, 0.063, and 0.066 μmol/mL, respectively) showed better activity.

From the above data, it has been revealed that:

1. Substitution on phenyl ring attached to nitrogen of amide group demonstrated better activity compared to unsubstituted counterpart.
2. Compounds having electron-withdrawing nitro group on phenyl ring showed an advantage over the corresponding electron-releasing methyl/ethyl group in most of the cases.
3. It has been observed that with increasing carbon chain present at C_4 of triazole ring showed improved antifungal activity.
4. Also, the presence of alkyl group on carbon having free hydroxyl group enhanced the antifungal activity.

Table 3 In vitro antioxidant activity of 1,4-disubstituted 1,2,3-triazoles (**5a**–**5t**)

Compound	$IC_{50} \pm SD$	Compound	$IC_{50} \pm SD$
5a	5.87 ± 0.95	**5k**	3.90 ± 0.45
5b	4.74 ± 0.75	**5l**	5.91 ± 1.24
5c	3.19 ± 0.59	**5m**	5.65 ± 0.87
5d	5.86 ± 0.94	**5n**	4.38 ± 0.58
5e	7.77 ± 1.37	**5o**	2.94 ± 0.47
5f	5.09 ± 0.74	**5p**	5.73 ± 0.91
5g	4.00 ± 0.64	**5q**	5.28 ± 0.62
5h	7.11 ± 1.29	**5r**	4.09 ± 0.61
5i	6.76 ± 1.12	**5s**	2.89 ± 0.51
5j	4.81 ± 0.68	**5t**	5.10 ± 0.87
Ascorbic acid	1.23 ± 0.55		

Values were the mean of three replicates ± SD

Antioxidant activity

The in vitro antioxidant activity of synthesized 1,4-disubstituted 1,2,3-triazoles was performed spectrophotometrically using 2,2-diphenyl-1-picrylhydrazyl (DPPH) free radical scavenging assay. Table 3 summarizes the radical scavenging activities of all compounds compared to ascorbic acid as standard. Compound **5s** was found to show good antioxidant potential with IC_{50} value of 2.89 ± 0.51 μg/mL. Compounds **5c, 5k**, and **5o** also showed good radical scavenging activity with IC_{50} value of 3.19 ± 0.59, 3.90 ± 0.45, and 2.94 ± 0.47 μg/mL, respectively.

From the above data it has been generalized that

1. Substitution on phenyl ring attached to nitrogen of amide group demonstrated better activity compared to unsubstituted counterpart.
2. Incorporation of ethyl group on phenyl ring attached to nitrogen of amide exhibited better activity than other corresponding substitutions.
3. It has been observed that with increasing carbon chain present at C_4 of triazole ring showed increasing antioxidant activity.
4. The activity data revealed that presence of alkyl group on carbon having free hydroxyl group decreases the antioxidant potential.
5. In most of the cases, presence of nitro group on

phenyl ring showed decreased antioxidant potential compared to triazoles having methyl/ethyl substitution on phenyl ring.

Docking studies

For determination of probable binding conformation of the tested compounds responsible for their antimicrobial activity, the docking studies of active molecules were carried out in the active site of well-known antibacterial drug target i.e., *E. coli* DNA gyrase (PDB ID: 1kzn) and antifungal drug target Lanosterol 14-α demethylase (PDB:4WMZ) obtained from RCSB protein data bank (Tables 4 and 5).

Hydroxyl oxygen of compound **5f** made hydrogen bond with Arg76. Triazole ring showed pi-alkyl interactions with Pro79 while methyl phenyl ring exhibited these types of interactions with Ala 47. The middle phenyl ring interacted with Ile78 and Ile90. Methyl group made an interaction pyramid with Val43, Val71, and Val167. In compound 5**g**, the overlapping conformation interacted with Arg76 through hydrogen bond with hydroxyl oxygen. One additional hydrogen bond was observed between carbonyl oxygen and Arg46 which might be the cause of its higher activity. Other hydrophobic interactions were almost same as for that 5**f**. Compound 5 **h** did not exhibited hydrogen bond interaction with Arg76 but with Arg 46 through its carbonyl oxygen atom. The calculated binding affinity for 5**f**, **5g**, and 5**h** was −7.2, −7.7, and −7.0 kcal/mol, respectively. The above-discussed binding interactions and conformations of these compounds are shown in Fig. 1. The docked conformations along with the co-crystallized ligand in the binding site of DNA gyrase are shown in Fig. 2.

In case of Lanosterol 14-α demethylase, hydroxyl oxygen of compound **5h** made hydrogen bond with Arg469. Nitro phenyl ring showed pi-sulfur, carbon-hydrogen bond interaction with Met508, pi-pi T-shaped interaction with Phe233, and carbon-hydrogen bond as well as pi-pi T-shaped interaction with His377. Triazole ring showed pi-pi T-shaped and carbon-hydrogen bond interactions with Tyr132. Compound 5**k** exhibited hydrogen bond interaction with Lys143 through hydroxyl oxygen. Pi-pi T-shaped interaction was shown with Phe233 through ethyl phenyl ring, with Tyr118 through middle phenyl ring and with Tyr132 through triazole ring. Pi-sulfur interaction was same as for that 5**h**. Other hydrophobic interactions were shown by ethyl groups with Pro230, His377, Ile471 and Lys143. In compound 5**l**, the overlapping conformation interacted with Arg469 through hydrogen bond with hydroxyl oxygen and with Tyr118 through pi donor hydrogen bond with carbonyl oxygen. Nitro phenyl ring showed pi-sulfur with Met508 and pi-pi T-shaped interaction with Phe233 and His377 while triazole ring showed pi-pi T-shaped interactions with Tyr132. Pi-donor hydrogen bond interaction was shown by Nitro group attached to phenyl ring with His377. In compound **5t**, His377 was involved in carbon-hydrogen bond interaction with nitro group, whereas triazole show pi-pi T-shaped interaction with Tyr132. The oxygen atom of hydroxyl and nitro group were engaged in hydrogen bond interaction with His468 and Tyr64, respectively. Nitro Phenyl ring show pi-sulfur interaction with Met508, pi-pi T-shaped interaction with Phe233 and pi-alkyl interaction with Pro230. Middle phenyl ring was engaged in hydrogen bonding with Tyr118. Therefore, it can be concluded that the compound under investigation may inhibit lanosterol 14-α demethylase via these interactions. The calculated binding affinity for 5**h, 5k**, 5**l**, and **5t** was −9.5, −9.6, −9.5, and −8.9 kcal/mol, respectively. The above-discussed binding interactions and conformations of these compounds are shown in Fig. 3.

Table 4 Docking score of docked molecules for antibactrial activity

S. No.	Name of molecule	Docking score (kcal/mol)
1	5f	−7.2
2	5g	−7.7
3	5h	−7.0

Table 5 Docking score of docked molecules for antifungal activity

S. No.	Name of molecule	Docking score (kcal/mol)
1	5h	−9.5
2	5k	−9.6
3	5l	−9.5
4	5t	−8.9

ADME studies

The Molinspiration online property calculation toolkit was used for determination of ADME (absorption, distribution, metabolism, elimination) parameters and drug likeliness of synthesized molecules which is a balance between molecular properties and structural features. There are five significant physicochemical parameters to calculate drug-likeness based on the Lipinski's rule. This rule predicts oral administration of candidate drug by obeying his rule i.e., log*P* (liphophilicity value) ≤ 5, molWt ≤ 500, number of H-bond acceptor (O and N atoms) ≤ 10 and number of H-bond donor group (-NH and -OH) ≤ 5. This includes molecule size, conformational flexibility, H-bond formation ability, hydrophobicity and electronic distribution for molecular properties. In the present study we have reported all the five necessary physicochemical parameters of the Lipinski's rule in Table 6. All the synthesized compounds have molecular weight ≤500, number of

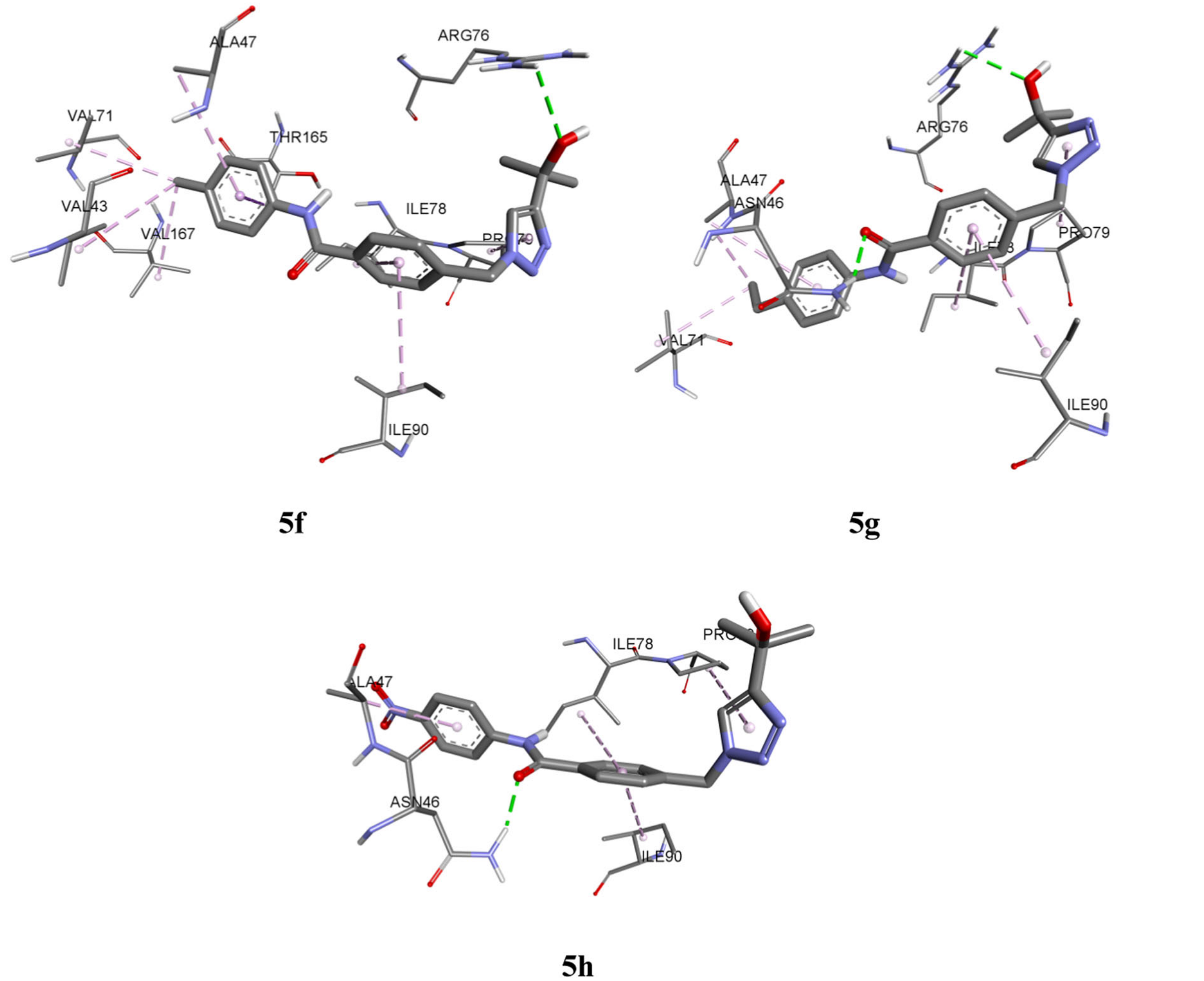

Fig. 1 Binding conformation and interactions of compounds **5f**, 5**g**, and 5**h** in the active site of DNA gyrase (Green dotted line: H-bond; Light pink dotted line: Hydrophobic interactions)

hydrogen bond acceptors ≤10, number of hydrogen bond donors ≤5, miLog $P \leq 5$. The number of rotatable bonds in compounds **(5a–5t)** clearly defines the flexible nature of compounds. The synthesized hybrids are expected to show good permeability across the cell membrane on the basis of values of miLog *P*. Percentage absorption was calculated as% ABS = 109-(0.345xTPSA). None of the compounds **(5a–5t)** violated Lipinski's rule-of-five, (All the studied compounds lie within the acceptable range of Lipinski's rule-of-five) thus making these derivatives as useful lead molecules for further study.

Materials and methods

General

Commercially available chemicals were used for the preparation of reactants **(3a–3d)**. The different chemicals used were 4-(bromomethyl)benzoyl bromide, different derivatives of aniline, Cell-CuI NPs, Na-ascorbate, propargyl alcohol derivatives and K_2CO_3. Silica plated aluminum gel (SIL G/UV254, ALUGRAM) were used to monitor the progress of reaction using thin-layer chromatography (TLC) and successful visualization was done under the UV light. Melting points (°C) were determined by open capillaries and the recorded melting points are reported as such. SHIMAZDU IR AFFINITY-I FTIR spectrophotometer was used for recording the IR spectra in the range of 400–4000 cm^{-1}. BRUKER AVANCE II 400 MHz spectrometer was used for interpreting the NMR spectra of the compounds using DMSO as solvent and chemical shifts (δ) were reported in parts per million downfield from the internal standard trimethylsilane (TMS) while coupling constant (J) values in Hertz (Hz). Bruker micro TOF Q-II spectrometer was used for recording the HRMS of compounds formed.

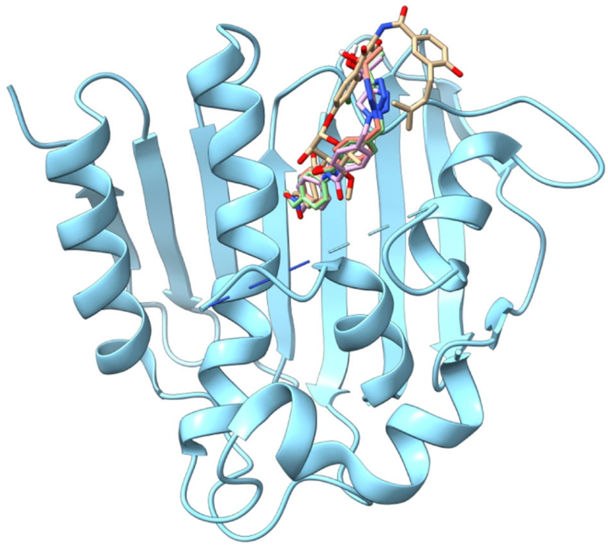

Fig. 2 Compound **5f** (light pink), **5g** (green), **5h** (brown), and co-crystalized ligand (pale yellowish brown) in the active site of *E. coli* DNA gyrase (Cartoon depiction)

Preparation of cellulose-supported cuprous iodide nanoparticles (Cell-CuI NPs)

Nanoparticles were prepared using method [38] reported by Chavan et al. To the stirred suspension of CuI (0.190 g, 1 mmol) in methanol (30 mL), microcrystalline cellulose (2 g) was added and stirring was continued for 12–14 h. The reaction contents were filtered and residue was washed repeatedly with methanol and finally with acetone. It was dried in air and then dried under vacuum for 6 h at 50–60 °C.

General procedure for the synthesis of 4-(bromomethyl)-N-arylbenzamides [39] (3a–3d)

Aromatic amines **(2a–2d)** (1.0 mmol) were dissolved in dichloromethane (15 mL) taken in a round bottom flask and potassium carbonate (2.0 mmol) was added to it. Then 4-(bromomethyl)benzoylbromide **(1)** (1.0 mmol) was added dropwise and the reaction mixture was stirred at 0–10 °C. After the completion of reaction, the product was extracted with dichloromethane (3 × 15 mL). Then solvent was evaporated under reduced pressure to obtain desired 4-(bromomethyl)-N-arylbenzamides **(3a–3d)**.

General procedure for the synthesis of 4-((4-(hydroxyalkyl)-1*H*-1,2,3-triazol-1-yl)methyl)-N-substituted benzamides (5a-5t)

4-(bromomethyl)-N-arylbenzamides **(3a–3d)** (1.0 mmol), terminal alkynes **(4a–4e)** (1.0 mmol) and sodium azide (2.0 mmol) were dissolved in water in a round bottom flask and cellulose-CuI NPs catalyst (100 mg) was added and the reaction mixture was allowed to stir for 6–10 h at 60-70 °C. After completion of reaction, ice-cold water and ammonia solution (15 mL) was added, the precipitated solid was filtered and recrystallized from ethyl acetate to yield the pure 1,4-disubstituted 1,2,3-triazoles **(5a–5t)**.

Characterization data of synthesized compounds

4-((4-(hydroxymethyl)-1*H*-1,2,3-triazol-1-yl)methyl)-N-phenylbenzamide (5a)

Appearance: white solid; yield: 81%; mp: 174–176 °C; FTIR (KBr): ν_{max} = 3334 (O–H str.), 3288 (N–H str.), 3138 (C–H str., triazole ring), 3072 (C–H str., aromatic ring), 2963 (C–H str., aliphatic), 1651 (C=O str., amide), 1543, 1438 (C=C str., aromatic ring) cm^{-1}; ^1H NMR (400 MHz, DMSO-d_6) δ 10.23 (s, 1H, N-H amide), 8.03 (s, 1H, C-H triazole), 7.91 (d, J = 4.0 Hz, 2H, ArH), 7.72 (d, J = 8.0 Hz, 2H, ArH), 7.41 (d, J = 4.0 Hz, 2H, ArH), 7.32–7.29 (m, 2H, ArH), 7.07–7.04 (m, 1H, ArH), 5.64 (s, 2H, NCH_2), 5.18 (t, J = 4.0 Hz, 1H, OH), 4.48 (d, J = 4.0 Hz, 2H, OCH_2); ^{13}C NMR (100 MHz, DMSO-d_6) δ 165.7 (C=O), 148.9 (C_4 triazole), 140.1, 139.6, 135.2, 129.1, 128.6, 128.4, 124.2, 123.5, 120.8 (C_5 triazole), 55.5, 52.8 (NCH_2); HRMS (*m/z*) calculated for $C_{17}H_{16}N_4O_2$ $[M + H]^+$: 309.1347, Found: 309.1248.

4-((4-(hydroxymethyl)-1*H*-1,2,3-triazol-1-yl)methyl)-N-(p-tolyl)benzamide (5b)

Appearance: white solid; yield: 79%; mp: 205–208 °C; FTIR (KBr): ν_{max} = 3382 (O–H str.), 3280 (N–H str.), 3136 (C–H str., triazole ring), 3091 (C–H str., aromatic ring), 2993 (C–H str., aliphatic), 1651 (C=O str., amide), 1535, 1435 (C=C str., aromatic ring) cm^{-1}; ^1H NMR (400 MHz, DMSO-d_6) δ 10.18 (s, 1H, N-H amide), 8.07 (s, 1H, C-H triazole), 7.93 (d, J = 8.0 Hz, 2H, ArH), 7.64 (d, J = 8.0 Hz, 2H, ArH), 7.44 (d, J = 8.0 Hz, 2H, ArH), 7.15 (d, J = 8.0 Hz, 2H, ArH), 5.68 (s, 2H, NCH_2), 5.22 (s, 1H, OH), 4.52 (s, 2H, OCH_2), 2.28 (s, 3H, CH_3); ^{13}C NMR (100 MHz, DMSO-d_6) δ 165.4 (C=O), 148.9 (C_4 triazole), 139.9, 137.0, 135.3, 133.1, 129.5, 128.5, 128.3, 123.5, 120.8 (C_5 triazole), 55.5, 52.7 (NCH_2), 20.9; HRMS (*m/z*) calculated for $C_{18}H_{18}N_4O_2$ $[M + H]^+$: 323.1503. Found: 323.1436.

N-(4-ethylphenyl)-4-((4-(hydroxymethyl)-1*H*-1,2,3-triazol-1-yl)methyl)benzamide (5c)

Appearance: white solid; yield: 82%; mp: 190–194 °C; FTIR (KBr): ν_{max} = 3348 (O–H str.), 3262 (N–H str.), 3116 (C–H str., triazole ring), 3058 (C–H str., aromatic ring), 2963 (C–H str., aliphatic), 1653 (C=O str., amide), 1527, 1430 (C = C str., aromatic ring) cm^{-1}; ^1H NMR (400 MHz,

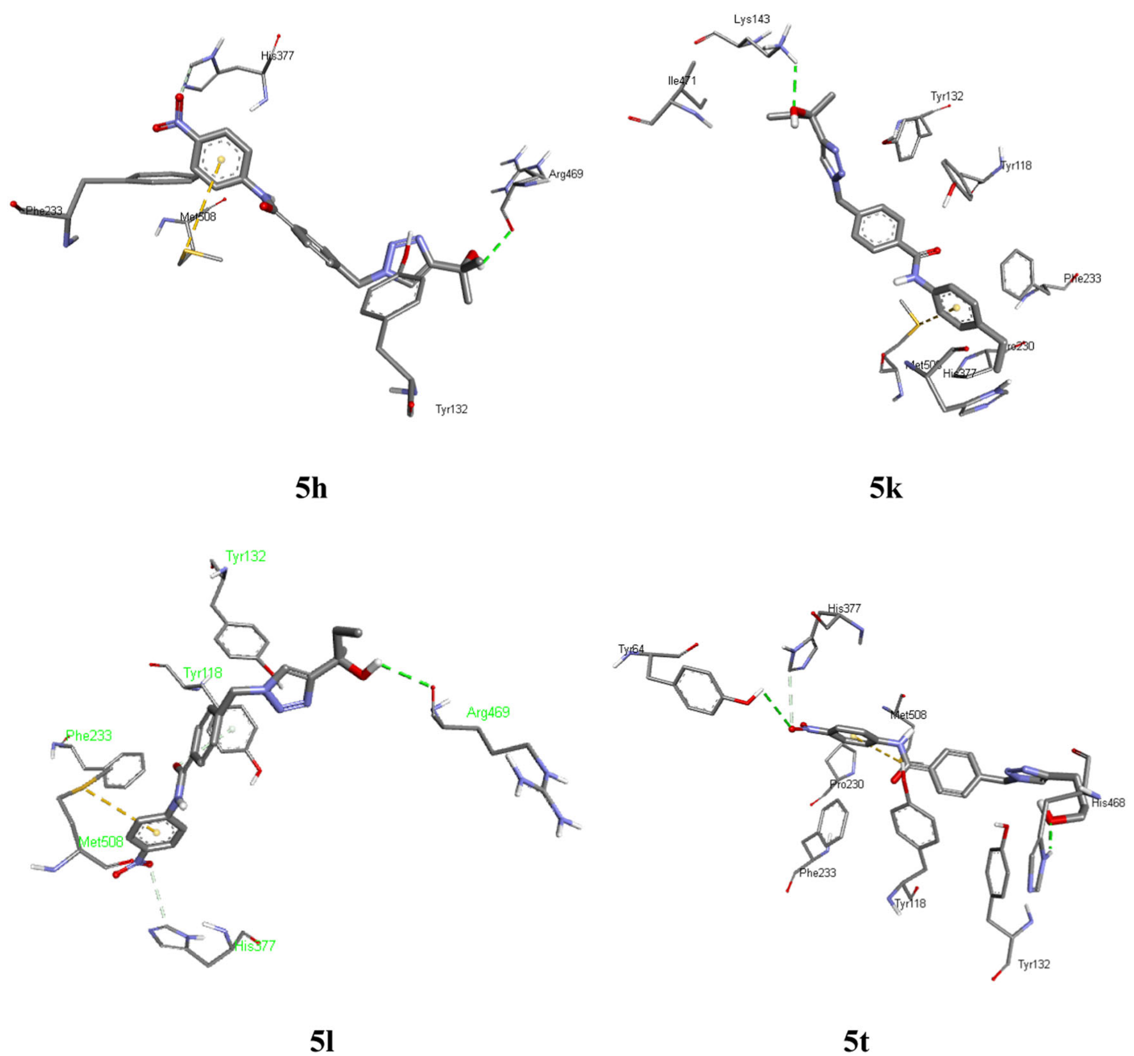

Fig. 3 Binding conformation and interactions of compounds **5h**, 5**k**, **5l**, and **5t** in the active site of antifungal target Lanosterol 14-α demethylase

DMSO-d_6) δ 10.23 (s, 1H, N-H amide), 8.08 (s, 1H, C-H triazole), 7.95 (d, $J = 8.0$ Hz, 2H, ArH), 7.67 (d, $J = 8.0$ Hz, 2H, ArH), 7.44 (d, $J = 8.0$ Hz, 2H, ArH), 7.18 (d, $J = 8.0$ Hz, 2H, ArH), 5.68 (s, 2H, NCH_2), 4.53 (s, 2H, -OCH_2), 2.57 (q, $J = 8.0$ Hz, 2H), 2.51 (s, 1H), 1.17 (t, $J = 8.0$ Hz, 3H); ^{13}C NMR (100 MHz, DMSO-d_6) δ 165.4 (C=O), 148.9 (C_4 triazole), 139.9, 139.6, 137.2, 135.2, 128.5, 128.3, 128.2, 123.5, 120.9 (C_5 triazole), 55.5, 52.7 (NCH_2), 28.1, 16.2; HRMS (*m/z*) calculated for $C_{19}H_{20}N_4O_2$ $[M + H]^+$: 337.1660. Found: 337.1576.

4-((4-(hydroxymethyl)-1*H*-1,2,3-triazol-1-yl)methyl)-N-(4-nitrophenyl)benzamide (5d)

Appearance: yellow solid; yield: 86%; mp: 264–265 °C; FTIR (KBr): $\nu_{max} = 3477$ (O–H str.), 3338 (N–H str.), 3136 (C–H str., triazole ring), 3078 (C–H str., aromatic ring), 2933 (C–H str., aliphatic), 1678 (C = O str., amide), 1543, 1438 (C=C str., aromatic ring) cm^{-1}; ^{1}H NMR (400 MHz, DMSO-d_6) δ 10.81 (s, 1H, N-H amide), 8.27 (d, $J = 8.0$ Hz, 2H, ArH), 8.08-8.03 (m, 3H, C-H triazole, ArH), 7.97 (d, $J = 8.0$ Hz, 2H, ArH), 7.48 (d, $J = 8.0$ Hz, 2H, ArH), 5.70 (s, 2H, NCH_2), 5.215 (t, $J = 4.0$ Hz, 1H, OH), 4.53 (d, $J = 4.0$ Hz, 2H, OCH_2); ^{13}C NMR (100 MHz, DMSO-d_6) δ 166.38 (C=O), 154.7, 148.9 (C_4 triazole), 145.8, 143.7, 142.9, 140.7, 136.6, 134.4, 133.5, 128.8, 128.7, 128.4, 127.6, 126.6, 125.3, 123.5, 120.3 (C_5 triazole), 55.5, 52.7 (NCH_2), 45.9, 21.2; HRMS (*m/z*) calculated for $C_{17}H_{15}N_5O_4$ $[M + H]^+$: 354.1197. Found: 354.1194.

4-((4-(2-hydroxypropan-2-yl)-1*H*-1,2,3-triazol-1-yl)methyl)-N-phenylbenzamide (5e)

Appearance: white solid; yield: 83%; mp: 238–241 °C; FTIR (KBr): $\nu_{max} = 3410$ (O–H str.), 3350 (N–H str.), 3145 (C–H str., triazole ring), 3059 (C–H str., aromatic ring),

Table 6 ADME parameters of synthesized 1,4-disubstituted 1,2,3-triazoles (**5a–5t**)

Compounds	% ABS	MW	miLogP	TPSA	N atoms	nOH	nOHNH	nRot bond	Volume
5a	81.38	308.34	1.92	80.04	23	6	2	5	276.92
5b	81.38	322.37	2.36	80.04	24	6	2	5	293.48
5c	81.38	336.39	2.83	80.04	25	6	2	6	310.29
5d	65.57	353.34	1.87	125.87	26	9	2	6	300.26
5e	81.38	336.39	2.73	80.04	25	6	2	5	309.75
5f	81.38	350.42	3.17	80.04	26	6	2	5	326.31
5g	81.38	364.45	3.64	80.04	27	6	2	6	343.11
5h	65.57	381.39	2.68	125.87	28	9	2	6	333.08
5i	81.38	350.42	3.23	80.04	26	6	2	6	326.55
5j	81.38	364.45	3.68	80.04	27	6	2	6	343.11
5k	81.38	378.48	4.14	80.04	28	6	2	7	359.91
5l	65.57	395.42	3.19	125.87	29	9	2	7	349.88
5m	81.38	322.37	2.12	80.04	24	6	2	6	293.72
5n	81.38	336.39	2.57	80.04	25	6	2	6	310.29
5o	81.38	350.42	3.04	80.04	26	6	2	7	327.09
5p	65.57	367.37	2.08	125.87	27	9	2	7	317.06
5q	81.38	336.39	2.40	80.04	25	6	2	7	310.53
5r	81.38	350.42	2.84	80.04	26	6	2	7	327.09
5s	81.38	364.45	3.31	80.04	27	6	2	8	343.89
5t	65.57	381.39	2.35	125.87	28	9	2	8	333.86

2978 (C–H str., aliphatic), 1654 (C=O str., amide), 1531, 1440 (C=C str., aromatic ring) cm^{-1}; ^{1}H NMR (400 MHz, DMSO-d_6) δ 10.29 (s, 1H, N-H amide), 7.97 (s, 3H, C-H triazole, ArH), 7.78-7.75 (m, 2H, ArH), 7.46 (d, $J = 8.0$ Hz, 2H, ArH), 7.35 (t, $J = 8.0$ Hz, 2H, ArH), 7.10 (t, $J = 8.0$ Hz, 1H, ArH), 5.65 (s, 2H, NCH_2), 5.12 (s, 1H, OH), 1.46 (s, 6H, $C(CH_3)_2$); ^{13}C NMR (100 MHz, DMSO-d_6) δ 165.6 (C=O), 156.7, 148.9 (C_4 triazole), 140.0, 135.2, 129.0, 128.6, 128.4, 124.1, 121.2, 120.8 (C_5 triazole), 67.5, 52.7 (NCH_2), 31.2; HRMS (*m/z*) calculated for $C_{19}H_{20}N_4O_2$ $[M + H]^+$: 337.1660. Found: 337.1582.

4-((4-(2-hydroxypropan-2-yl)-1*H*-1,2,3-triazol-1-yl)methyl)-N-(p-tolyl)benzamide (5f)

Appearance: white solid; yield: 87%; mp: 230–234 °C; FTIR (KBr): $\nu_{max} = 3334$ (O–H str.), 3284 (N–H str.), 3118 (C–H str., triazole ring), 3061 (C–H str., aromatic ring), 2972 (C–H str., aliphatic), 1658 (C=O str., amide), 1533, 1431 (C = C str., aromatic ring) cm^{-1}; ^{1}H NMR (400 MHz, DMSO-d_6) δ 10.18 (s, 1H, N-H amide), 7.96 (s, 1H, C-H triazole), 7.93 (d, $J = 8.0$ Hz, 2H, ArH), 7.64 (s, 2H, ArH), 7.46 (d, $J = 8.0$ Hz, 2H, ArH), 7.15 (d, $J = 8.0$ Hz, 2H, ArH), 5.64 (s, 2H, NCH_2), 5.13 (s, 1H, OH), 2.28 (s, 3H, CH_3), 1.45 (s, 6H); ^{13}C NMR (100 MHz, DMSO-d_6) δ 165.6 (C=O), 151.4, 148.6 (C_4 triazole), 143.9, 136.5, 129.5, 128.5, 128.2, 125.9, 124.5, 118.6 (C_5 triazole), 115.2, 54.1, 52.7 (NCH_2), 27.3; HRMS (*m/z*) calculated for $C_{20}H_{22}N_4O_2$ $[M + H]^+$: 351.1816. Found: 351.1749.

N-(4-ethylphenyl)-4-((4-(2-hydroxypropan-2-yl)-1*H*-1,2,3-triazol-1-yl)methyl)benzamide (5g)

Appearance: white solid; yield: 84%; mp: 219–221 °C; FTIR (KBr): $\nu_{max} = 3359$ (O–H str.), 3275 (N–H str.), 3114 (C–H str., triazole ring), 3062 (C–H str., aromatic ring), 2963 (C–H str., aliphatic), 1653 (C=O str., amide), 1529, 1427 (C=C str., aromatic ring) cm^{-1}; ^{1}H NMR (400 MHz, DMSO-d_6) δ 10.29 (s, 1H, N-H amide), 7.97 (s, 3H, C-H triazole, ArH), 7.78-7.75 (m, 2H, ArH), 7.46 (d, $J = 8.0$ Hz, 2H, ArH), 7.35 (t, $J = 8.0$ Hz, 2H, ArH), 5.65 (s, 2H, NCH_2), 5.12 (s, 1H, OH), 2.57 (q, $J = 8.0$ Hz, 2H), 1.46 (s, 6H, $C(CH_3)_2$), 1.17 (t, $J = 8.0$ Hz, 3H). ^{13}C NMR (100 MHz, DMSO-d_6) δ 165.3 (C=O), 155.6, 148.4 (C_4 triazole), 140.0, 139.5, 137.2, 135.1, 128.6, 128.2, 122.0, 120.9 (C_5 triazole), 70.2, 52.7 (NCH_2), 31.2, 28.1, 16.2. HRMS (*m/z*) calculated for $C_{21}H_{24}N_4O_2$ $[M + H]^+$: 365.1973. Found: 365.1869.

4-((4-(2-hydroxypropan-2-yl)-1*H*-1,2,3-triazol-1-yl)methyl)-N-(4-nitrophenyl)benzamide (5h)

Appearance: yellow solid; yield: 89%; mp: 230–231 °C; FTIR (KBr): $\nu_{max} = 3360$ (O–H str.), 3261 (N–H str.), 3118 (C–H str., triazole ring), 3089 (C–H str., aromatic ring), 2987 (C–H str., aliphatic), 1670 (C=O str., amide), 1548, 1440 (C=C str., aromatic ring) cm^{-1}; ^1H NMR (400 MHz, DMSO-d_6) δ 10.16 (s, 1H, N-H amide), 8.22 (s, 1H, ArH), 7.83 (s, 2H, C-H triazole, ArH), 7.60 (s, 2H, ArH), 7.31 (d, $J = 8.0$ Hz, 3H, ArH), 6.88 (s, 1H, ArH), 5.61 (s, 2H, NCH_2), 4.62 (s, 1H, OH), 2.46 (s, 6H, $C(CH_3)_2$); ^{13}C NMR (100 MHz, DMSO-d_6) δ 165.3 (C=O), 151.8, 148.5 (C_4 triazole), 141.7, 135.2, 132.5, 128.5, 128.3, 125.2, 124.9, 122.6, 118.9 (C_5 triazole), 114.2, 110.8, 55.7, 52.9 (NCH_2), 26.9; HRMS (*m/z*) calculated for $C_{19}H_{19}N_5O_4$ $[M + H]^+$: 382.1510. Found: 382.1446.

4-((4-(2-hydroxybutan-2-yl)-1*H*-1,2,3-triazol-1-yl)methyl)-N-phenylbenzamide (5i)

Appearance: white solid; yield: 82%; mp: 204–206 °C; FTIR (KBr): $\nu_{max} = 3346$ (O–H str.), 3286 (N–H str.), 3138 (C–H str., triazole ring), 3072 (C–H str., aromatic ring), 2972 (C–H str., aliphatic), 1653 (C = O str., amide), 1531, 1440 (C=C str., aromatic ring) cm^{-1}; ^1H NMR (400 MHz, DMSO-d_6) δ 10.22 (s, 1H, N-H amide), 7.91–7.88 (m, 3H, C-H triazole, ArH), 7.72–7.70 (m, 2H, ArH), 7.39 (d, $J = 4.0$ Hz, 2H, ArH), 7.33–7.28 (m, 2H, ArH), 7.08–7.05 (m, 1H, ArH), 5.61 (s, 2H, NCH_2), 4.97 (s, 1H, OH), 1.71–1.68 (m, 2H,), 1.38 (s, 3H, CH_3), 0.68 (t, $J = 4.0$ Hz, 3H, CH_2CH_3); ^{13}C NMR (100 MHz, DMSO-d_6) δ 165.7 (C=O), 155.7, 147.9 (C_4 triazole), 140.2 139.5, 135.2, 129.2, 128.6, 128.4, 124.3, 122.1, 120.8 (C_5 triazole), 70.3, 52.7 (NCH_2), 35.9, 28.7, 8.8; HRMS (*m/z*) calculated for $C_{20}H_{22}N_4O_2$ $[M + H]^+$: 351.1816. Found: 351.1719.

4-((4-(2-hydroxybutan-2-yl)-1*H*-1,2,3-triazol-1-yl)methyl)-N-(p-tolyl)benzamide (5j)

Appearance: white solid; yield: 88%; mp: 258–261 °C; FTIR (KBr): $\nu_{max} = 3340$ (O–H str.), 3290 (N–H str.), 3136 (C–H str., triazole ring), 3068 (C–H str., aromatic ring), 2897 (C–H str., aliphatic), 1662 (C=O str., amide), 1514, 1431 (C=C str., aromatic ring) cm^{-1}; ^1H NMR (400 MHz, DMSO-d_6) δ 10.18 (s, 1H, N-H amide), 8.07 (s, 1H, C-H triazole), 7.93 (d, $J = 8.0$ Hz, 2H, ArH), 7.64 (d, $J = 8.0$ Hz, 2H, ArH), 7.44 (d, $J = 8.0$ Hz, 2H, ArH), 7.15 (d, $J = 8.0$ Hz, 2H, ArH), 5.61 (s, 2H, NCH_2), 4.97 (s, 1H, OH), 2.28 (s, 3H, CH_3), 1.71–1.68 (m, 2H), 1.38 (s, 3H, CH_3), 0.68 (t, $J = 4.0$ Hz, 3H, -CH_2CH_3); ^{13}C NMR (100 MHz, DMSO-d_6) δ 165.4 (C=O), 148.9 (C_4 triazole), 139.9, 137.0, 135.3, 133.1, 129.5, 128.5, 128.3, 123.5, 120.8 (C_5 triazole), 70.3, 52.7 (NCH_2), 35.9, 28.7, 20.9; HRMS (*m/z*) calculated for $C_{21}H_{24}N_4O_2$ $[M + H]^+$: 365.1973. Found: 365.1877.

N-(4-ethylphenyl)-4-((4-(2-hydroxybutan-2-yl)-1*H*-1,2,3-triazol-1-yl)methyl)benzamide (5k)

Appearance: white solid; yield: 81%; mp: 216–218 °C; FTIR (KBr): $\nu_{max} = 3346$ (O–H str.), 3243 (N–H str.), 3124 (C–H str., triazole ring), 3042 (C–H str., aromatic ring), 2966 (C–H str., aliphatic), 1654 (C=O str. amide), 1522, 1458 (C=C str., aromatic ring); ^1H NMR (400 MHz, DMSO-d_6) δ 10.26 (s, 1H, N-H amide), 7.97-7.94 (m, 3H, C-H triazole, ArH), 7.67 (d, $J = 8.0$ Hz, 2H, ArH), 7.44 (d, $J = 8.0$ Hz, 2H, ArH), 7.17 (d, $J = 8.0$ Hz, 2H, ArH), 5.65 (s, 2H, NCH_2), 4.99 (s, 1H, OH), 2.57 (q, $J = 8.0$ Hz, 2H), 1.75–1.70 (m, 2H,), 1.41 (s, 3H, CH_3), 1.17 (t, $J = 4.0$ Hz, 3H), 0.72 (t, $J = 4.0$ Hz, 3H); ^{13}C NMR (100 MHz, DMSO-d_6) δ 165.3 (C=O), 155.6, 148.2 (C_4 triazole), 140.0, 139.5, 137.2, 135.1, 128.6, 128.2, 122.0, 120.9 (C_5 triazole), 70.2, 52.7 (NCH_2), 35.9, 28.7, 28.1, 16.2, 8.8; HRMS (*m/z*) calculated for $C_{22}H_{26}N_4O_2$ $[M + H]^+$: 379.2129. Found: 379.2027.

4-((4-(2-hydroxybutan-2-yl)-1*H*-1,2,3-triazol-1-yl)methyl)-N-(4-nitrophenyl)benzamide (5l)

Appearance: yellow solid; yield: 89%; mp: 191–195 °C; FTIR (KBr): $\nu_{max} = 3360$ (O–H str.), 3267 (N–H str.), 3143 (C–H str., triazole ring), 3078 (C–H str., aromatic ring), 2966 (C–H str., aliphatic), 1683 (C=O str., amide), 1544, 1462 (C=C str., aromatic ring) cm^{-1}; ^1H NMR (400 MHz, DMSO-d_6) δ 10.81 (s, 1H, N-H amide), 8.27 (d, $J = 8.0$ Hz, 2H, ArH), 8.08-8.03 (m, 3H, C-H triazole, ArH), 7.97 (d, $J = 8.0$ Hz, 2H, ArH), 7.48 (d, $J = 8.0$ Hz, 2H, ArH), 5.61 (s, 2H, NCH_2), 4.97 (s, 1H, OH), 1.71-1.68 (m, 2H), 1.38 (s, 3H, CH_3), 0.68 (t, $J = 4.0$ Hz, 3H, CH_2CH_3); ^{13}C NMR (100 MHz, DMSO-d_6) δ 166.4 (C=O), 154.7, 148.9 (C_4 triazole), 145.8, 143.7, 142.9, 140.7, 136.6, 134.4, 133.5, 128.8, 128.7, 128.4, 127.9, 126.6, 125.3, 123.5, 120.3 (C_5 triazole), 70.3, 52.7 (NCH_2), 35.9, 28.7; HRMS (*m/z*) calculated for $C_{20}H_{21}N_5O_4$ $[M + H]^+$: 396.1667. Found: 396.1564.

4-((4-(2-hydroxyethyl)-1*H*-1,2,3-triazol-1-yl)methyl)-N-phenylbenzamide (5m)

Appearance: white solid; yield: 90%; mp: 255–257 °C; FTIR (KBr): $\nu_{max} = 3336$ (O–H str.), 3290 (N–H str.), 3126 (C–H str., triazole ring), 3062 (C–H str., aromatic ring), 2937 (C–H str., aliphatic), 1653 (C=O str., amide), 1529, 1431 (C=C str., aromatic ring) cm^{-1}; ^1H NMR (400 MHz, DMSO-d_6) δ 10.21 (s, 1H, N-H amide), 7.92 (s, 1H, C-H triazole), 7.89 (d, $J = 8.0$ Hz, 2H, ArH), 7.715 (d, $J = 4.0$ Hz, 2H, ArH), 7.39 (d, $J = 8.0$ Hz, 2H, ArH), 7.31 (t, $J = 8.0$ Hz, 2H, ArH), 7.08–7.04 (m, 1H, ArH), 5.61 (s, 2H, NCH_2), 4.68 (t, $J = 4.0$ Hz, 1H, OH), 3.61–3.55 (m, 2H, OCH_2), 2.73 (t,

$J = 4.0$ Hz, 2H); ^{13}C NMR (100 MHz, DMSO-d_6) δ 165.8 (C=O), 148.7 (C_4 triazole), 142.2, 140.1, 136.5, 135.5, 130.9, 129.3, 129.2, 128.3, 125.1, 120.9 (C_5 triazole), 51.2, 50.8 (NCH_2), 29.9; HRMS (*m/z*) calculated for $C_{18}H_{18}N_4O_2$ $[M + H]^+$: 323.1503. Found: 323.1433.

4-((4-(2-hydroxyethyl)-1*H*-1,2,3-triazol-1-yl)methyl)-N-(p-tolyl)benzamide (5n)

Appearance: white solid; yield: 83%; mp: 265–266 °C; FTIR (KBr): $\nu_{max} = 3384$ (O–H str.), 3298 (N–H str.), 3142 (C–H str., triazole ring), 3072 (C–H str., aromatic ring), 2937 (C–H str., aliphatic), 1651 (C=O str. amide), 1525, 1429 (C=C str., aromatic ring) cm^{-1}; ^{1}H NMR (400 MHz, DMSO-d_6) δ 10.16 (s, 1H, N-H amide), 7.95 (s, 1H, C-H triazole), 7.92 (d, $J = 8.0$ Hz, 2H, ArH), 7.63 (d, $J = 8.0$ Hz, 2H, ArH), 7.42 (d, $J = 8.0$ Hz, 2H, ArH), 7.15 (d, $J = 8.0$ Hz, 2H, ArH), 5.64 (s, 2H, NCH_2), 4.71 (t, $J = 4.0$ Hz, 1H, OH), 3.66-3.59 (m, 2H, OCH_2), 2.77 (t, $J = 8.0$ Hz, 2H), 2.28 (s, 3H, CH_3); ^{13}C NMR (100 MHz, DMSO-d_6) δ 186.1 (C=O), 147.3 (C_4 triazole), 140.3, 136.9, 135.3, 133.5, 129.5, 128.5, 128.3, 120.8 (C_5 triazole), 60.7, 58.4 (NCH_2), 29.6, 20.9; HRMS (*m/z*) calculated for $C_{19}H_{20}N_4O_2$ $[M + H]^+$: 337.1660. Found: 337.1582.

N-(4-ethylphenyl)-4-((4-(2-hydroxyethyl)-1*H*-1,2,3-triazol-1-yl)methyl)benzamide (5o)

Appearance: white solid; yield: 86%; mp: 178–181 °C; FTIR (KBr): $\nu_{max} = 3412$ (O–H str.), 3344 (N–H str.), 3113 (C–H str., triazole ring), 3052 (C–H str. aromatic ring), 2963 (C–H str., aliphatic), 1646 (C = O str., amide), 1527, 1437 (C=C str., aromatic ring) cm^{-1}; ^{1}H NMR (400 MHz, DMSO-d_6) δ 10.22 (s, 1H, N-H amide), 7.95 (d, $J = 8.0$ Hz, 3H, C-H triazole, ArH), 7.67 (d, $J = 8.0$ Hz, 2H, ArH), 7.42 (d, $J = 8.0$ Hz, 2H, ArH), 7.16 (d, $J = 8.0$ Hz, 2H, ArH), 5.65 (s, 2H, NCH_2), 4.75 (s, 1H, OH), 3.63 (s, 2H), 2.78 (t, $J = 4.0$ Hz, 2H), 2.57 (q, $J = 8.0$ Hz, 2H), 1.17 (t, $J = 8.0$ Hz, 3H); ^{13}C NMR (100 MHz, DMSO-d_6) δ 165.4 (C=O), 147.5 (C_4 triazole), 145.3, 139.9, 139.6, 137.2, 135.2, 128.5, 128.2, 123.2, 120.9 (C_5 triazole), 60.8, 52.7 (NCH_2), 29.6, 28.1, 16.2; HRMS (*m/z*) calculated for $C_{20}H_{22}N_4O_2$ $[M + H]^+$: 351.1816. Found: 351.1737.

4-((4-(2-hydroxyethyl)-1*H*-1,2,3-triazol-1-yl)methyl)-N-(4-nitrophenyl)benzamide (5p)

Appearance: yellow solid; yield: 87%; mp: 268–272 °C; FTIR (KBr): $\nu_{max} = 3356$ (O–H str.), 3280 (N–H str.), 3149 (C–H str., triazole ring), 3095 (C–H str., aromatic ring), 2933 (C–H str., aliphatic), 1680 (C=O str. amide), 1546, 1463 (C=C str., aromatic ring) cm^{-1}; ^{1}H NMR (400 MHz, DMSO-d_6) δ 10.82 (s, 1H, N-H amide), 8.28 (d, $J = 8.0$ Hz, 3H, ArH), 8.07-8.03 (d, $J = 8.0$ Hz, 2H, C-H triazole, ArH), 8.00-7.94 (m, 2H, ArH), 7.52 (d, $J = 8.0$ Hz, 1H, ArH), 7.46 (d, $J = 8.0$ Hz, 1H, ArH), 6.68 (d, $J = 8.0$ Hz, 1H, ArH), 5.67 (s, 2H, NCH_2), 4.71 (t, $J = 8.0$ Hz, 1H), 3.65–3.60 (m, 2H), 2.79–2.73 (m, 2H); ^{13}C NMR (100 MHz, DMSO-d_6) δ 166.5 (C=O), 166.4, 154.7, 148.8 (C_4 triazole), 145.9, 145.3, 143.7, 142.9, 140.8, 136.6, 134.4, 133.5, 128.8, 128.7, 128.4, 127.6, 126.6, 125.3, 123.2, 120.3 (C_5 triazole), 120.2, 60.8, 52.7 (NCH_2), 45.9, 29.6; HRMS (*m/z*) calculated for $C_{18}H_{17}N_5O_4$ $[M + H]^+$: 368.1354. Found: 368.1246.

4-((4-(3-hydroxypropyl)-1*H*-1,2,3-triazol-1-yl)methyl)-N-phenylbenzamide (5q)

Appearance: white solid; yield: 82%; mp: 238–241 °C; FTIR (KBr): $\nu_{max} = 3342$ (O–H str.), 3286 (N–H str.), 3129 (C–H str., triazole ring), 3064 (C–H str., aromatic ring), 2937 (C–H str., aliphatic), 1651 (C=O str. amide), 1533, 1435 (C=C str., aromatic ring) cm^{-1}; ^{1}H NMR (400 MHz, DMSO-d_6) δ 10.20 (s, 1H, N-H amide), 7.92–7.88 (m, 2H, C-H triazole, ArH), 7.85 (d, $J = 8.0$ Hz, 1H, ArH), 7.72 (d, $J = 8.0$ Hz, 2H, ArH), 7.38 (d, $J = 4.0$ Hz, 1H, ArH), 7.33–7.28 (m, 2H, ArH), 7.08–7.04 (m, 1H, ArH), 7.01–6.98 (m, 1H, ArH), 5.60 (s, 2H, NCH_2), 4.46 (t, $J = 4.0$ Hz, 1H, OH), 3.41–3.35 (m, 2H), 1.72–1.66 (m, 2H), 1.20 (s, 2H); ^{13}C NMR (100 MHz, DMSO-d_6) δ 165.7 (C=O), 148.9 (C_4 triazole), 140.1, 139.6, 135.2, 129.1, 128.6, 128.4, 124.2, 123.5, 120.8 (C_5 triazole), 60.4, 52.7 (NCH_2), 32.7, 22.1; HRMS (*m/z*) calculated for $C_{19}H_{20}N_4O_2$ $[M + H]^+$: 337.1660. Found: 337.1568.

4-((4-(3-hydroxypropyl)-1*H*-1,2,3-triazol-1-yl)methyl)-N-(p-tolyl)benzamide (5r)

Appearance: white solid; yield: 87%; mp: 225–226 °C; FTIR (KBr): $\nu_{max} = 3351$ (O–H str.), 3268 (N–H str.), 3115 (C–H str., triazole ring), 3062 (C–H str., aromatic ring), 2946 (C–H str., aliphatic), 1647 (C=O str., amide), 1530, 1432 (C=C str., aromatic ring) cm^{-1}; ^{1}H NMR (400 MHz, DMSO-d_6) δ 10.16 (s, 1H, N-H amide), 7.93 (d, $J = 8.0$ Hz, 3H, C-H triazole, ArH), 7.64 (d, $J = 8.0$ Hz, 2H, ArH), 7.41 (d, $J = 8.0$ Hz, 2H, ArH), 7.15 (d, $J = 8.0$ Hz, 2H, ArH), 5.64 (s, 2H, NCH_2), 4.50 (t, $J = 4.0$ Hz, 1H, OH), 3.43 (dd, $J = 12.0$, 8.0 Hz, 2H, OCH_2), 2.65 (t, $J = 8.0$ Hz, 2H), 2.28 (s, 3H, CH_3), 1.75–1.72 (m, 2H); ^{13}C NMR (100 MHz, DMSO-d_6) δ 165.4 (C=O), 147.7 (C_4 triazole), 140.0, 137.0, 135.2, 133.1, 129.4, 128.5, 128.1, 122.6, 120.8 (C_5 triazole), 60.5, 52.7 (NCH_2), 32.7, 22.1, 20.9; HRMS (*m/z*) calculated for $C_{20}H_{22}N_4O_2$ $[M + H]^+$: 351.1816. Found: 351.1726.

N-(4-ethylphenyl)-4-((4-(3-hydroxypropyl)-1*H*-1,2,3-triazol-1-yl)methyl)benzamide (5s)

Appearance: white solid; yield: 84%; mp: 190–193 °C; FTIR (KBr): ν_{max} = 3349 (O–H str.), 3278 (N–H str.), 3117 (C–H str., triazole ring), 3061 (C–H str., aromatic ring), 2963 (C–H str., aliphatic), 1648 (C=O str. amide), 1529, 1426 (C = C str., aromatic ring) cm^{-1}; ^{1}H NMR (400 MHz, DMSO-d_6) δ 10.23 (s, 1H, CONH), 7.97–7.95 (m, 3H, C-H triazole, ArH), 7.68 (d, *J* = 8.0 Hz, 2H, ArH), 7.41 (d, *J* = 8.0 Hz, 2H, ArH), 7.18 (d, *J* = 8.0 Hz, 2H, ArH), 5.64 (s, 2H, NCH_2), 4.53 (s, 1H, OH), 3.45–3.40 (m, 2H), 2.65 (t, *J* = 8.0 Hz, 2H), 2.57 (q, *J* = 7.5 Hz, 2H), 1.78–1.69 (m, 2H), 1.17 (t, *J* = 8.0 Hz, 3H); ^{13}C NMR (100 MHz, DMSO-d_6) δ 165.4 (C=O), 147.7 (C_4 triazole), 140.1, 139.6, 137.2, 135.1, 128.5, 128.2, 128.1, 122.6, 120.9 (C_5 triazole), 60.4, 52.7 (NCH_2), 32.7, 28.1, 22.1, 16.2; HRMS (*m/z*) calculated for $C_{21}H_{24}N_4O_2$ $[M + H]^+$: 365.1973. Found: 365.1887.

4-((4-(3-hydroxypropyl)-1*H*-1,2,3-triazol-1-yl)methyl)-N-(4-nitrophenyl)benzamide (5t)

Appearance: yellow solid; yield: 86%; mp: 268–270 °C; FTIR (KBr): ν_{max} = 3368 (O–H str.), 3263 (N–H str.), 3112 (C–H str., triazole ring), 3061 (C–H str., aromatic ring), 2940 (C–H str., aliphatic), 1659 (C = O str., amide), 1542, 1458 (C=C str., aromatic ring) cm^{-1}; ^{1}H NMR (400 MHz, DMSO-d_6) δ 10.89 (s, 1H, N-H amide), 8.27 (d, *J* = 8.0 Hz, 2H, ArH), 8.08 (d, *J* = 8.0 Hz, 2H, ArH), 7.98 (t, *J* = 8.0 Hz, 3H, ArH), 7.44 (d, *J* = 8.0 Hz, 2H, ArH), 5.66 (s, 2H, NCH_2), 4.53 (s, 1H, OH), 2.65–2.63 (m, 2H, OCH_2), 2.51 (broad singlet, 2H), 1.74–1.72 (m, 2H,-OCH_2CH_2); ^{13}C NMR (100 MHz, DMSO-d_6) δ 166.4 (C=O), 147.7 (C_4 triazole), 145.9, 142.9, 140.8, 134.3, 128.9, 128.3, 125.2, 122.7, 120.3 (C_5 triazole), 60.4, 52.7 (NCH_2), 32.7, 22.1; HRMS (*m/z*) calculated for $C_{19}H_{19}N_5O_4$ $[M + H]^+$: 382.1510. Found: 382.1440.

General procedure for in vitro antimicrobial evaluation

Two Gram-positive bacterial strains- *Staphylococcus gordonii* (MTCC 2695), *Bacillus subtilis* (MTCC 441) and two Gram-negative bacterial strain- *Escherichia coli* (MTCC 1231), *Klebsiella pneumoniae* (NCDC 138) were used for in vitro antibacterial screening, *Candida albicans* (MTCC 183) and *Rhizopus oryzae* were used for in vitro antifungal screening of synthesized triazole derivatives by serial dilution technique [40]. To get the stock solution of 200 µg/mL concentration, 2.0 mg of synthesized compound was dissolved in 10 mL of dimethylsulfoxide. Fresh nutrient broth and Fresh sabouraud dextrose were used as a culture media for bacterial and fungal strains, respectively. Ciprofloxacin and Fluconazole were used as standard against bacterial and fungal strains, respectively. Dimethylsulfoxide was used as solvent control. Initially, 1 mL of culture media was taken in each test tube and 1 mL of stock solution was added in one test tube to get the solution of 100 µg/mL concentration. Further, the concentration of 50–3.12 µg/ml were also obtained through serial dilution technique. After that, 0.1 mL of respective microorganism in sterile saline was inoculated in each test tube and then incubated at 37 ± 1 °C for 24 h.

General procedure for in vitro antioxidant evaluation

The antioxidant activities were carried out by following the procedure as reported by Kaushik et al. [41]. The in vitro antioxidant activity of synthesized compounds was performed spectrophotometrically using 2,2-diphenyl-1-picrylhydrazyl (DPPH) free radical scavenging assay. Stock solutions of the compounds (100 µg/mL) were prepared in methanol and diluted to different concentrations in the range of 20–100 µg/mL in methanol. Methanol, DPPH solution and standard drug were used as blank, control and reference respectively. Solution of organic compounds were taken in test tubes (2 mL) and then freshly prepared DPPH solution (1 mL) (0.004 g DPPH in 100 mL methanol) was added to every test tube. The samples were kept in the dark for 30 min after which absorbance was read against a blank at 517 nm (at an absorption maximum of DPPH) with UV–Visible spectrophotometer and the percentage of scavenging activity was calculated. The percentage of radical scavenging activity (RSA%) (I%) of the tested compounds was calculated according to the following equation:

$$\mathrm{RSA\%} = (\mathrm{A_0} - \mathrm{A_1})/\mathrm{A_0} \times 100$$

where A_0 is the absorbance of the control reaction and A_1 is the absorbance of the test sample.

Docking details

The docking protocols were followed as per procedure followed by Lat et al. [42]. Marvin Sketch [43] was used for drawing chemical structures, their standardization and 3D optimization. The protein preparation task was accomplished with the help of UCSF Chimera [44] and docking studies were executed with Autodock Vina software in the binding site of enzyme E. coli DNA Gyrase (pdb id: 1KZN) and antifungal drug target Lanosterol 14-α demethylase (PDB:4WMZ) retrieved from protein data bank. The docking simulation of co-crystallized ligand was done and the resulting most favorable docking conformation was within RMSD value of 2 Å with the co-crystallized conformation of Clorobiocin. Therefore, same protocols were used in the docking study of target compounds. The visualization of the results was performed with the help of Discovery Studio Visualizer [45] and Chimera X [46].

ADME studies

The in silico pharmacokinetics analysis of synthesized compounds was carried out by following procedure as given by Sharma et al. [47] using Molinspiration online property calculation toolkit. The online tool of molinspiration server is written in JAVA. There are five significant physico-chemical parameters to calculate drug-likeness based on the Lipinski rule. This rule predicts the oral administration of candidate drug by obeying this rule. It is a balance between molecular properties and structural features. It includes molecule size, conformational flexibility, H-bond formation ability, hydrophobicity and electronic distribution for molecular properties. In the present study, we have obtained all the four necessary physicochemical parameters of the Lipinski rule (Table 6). The absorption ability (%Abs) was calculated using% Absorption = 109−(0.345 × TPSA).

Conclusion

Here, we have synthesized 1,4-disubstituted 1,2,3-triazoles with amide-hydroxyl functionality **(5a–5t)** by treating 4-(bromomethyl)-N-arylbenzamide derivatives **(3a–3d)** with different terminal alkynes **(4a–4e)** using Cell-CuI NPs and evaluated for in vitro antimicrobial and antioxidant activities. Majority of the synthesized compounds exhibited moderate to potent antimicrobial and antioxidant activity. Docking studies of most active compounds exhibited good binding energy with ligand-receptor complexes and ADME properties also supported antimicrobial potency. In fact, it was noticed that the most active compounds **5h** and **5l** may be used as lead compounds for the further development of antimicrobial compounds. From these studies compound **5s** has pinpointed as most promising compound which show intense antioxidant potential than the other compounds.

Acknowledgements Authors are highly thankful to the Council of Scientific and Industrial Research (CSIR) for financial assistance.

Compliance with ethical standards

Conflict of interest The authors declare no competing interests.

References

1. Okusu H, Ma D, Nikaido H. AcrAB efflux pump plays a major role in the antibiotic resistance phenotype of Escherichia coli multiple-antibiotic-resistance (Mar) mutants. J Bacteriol. 1996;178:306 https://doi.org/10.1128/jb.178.1.306-308.1996
2. Isturiz RE. Optimizing antimicrobial prescribing. Int J Antimicrob Agents. 2010;36:S19–S22. https://doi.org/10.1016/S0924-8579(10)70006-6
3. Peterson E, Kaur P. Antibiotic resistance mechanisms in bacteria: relationships between resistance determinants of antibiotic producers, environmental bacteria, and clinical pathogens. Front Microbiol. 2018;9:2928 https://doi.org/10.3389/fmicb.2018.02928
4. Guyton KZ, Kensler TW. Oxidative mechanism in carcinogenesis. Br Med Bull. 1993;49:523–44. https://doi.org/10.1093/oxfordjournals.bmb.a072628
5. Singh A, Fong G, Liu J, Wu YH, Chang K, Park W, et al. Synthesis and preliminary antimicrobial analysis of isatin−ferrocene and isatin−ferrocenyl chalcone conjugates. ACS Omega. 2018;3:5808–5813. https://doi.org/10.1021/acsomega.8b00553
6. Recnik LM, Kandioller W, Mindt TL. 1, 4-Disubstituted 1, 2, 3-triazoles as amide bond surrogates for the stabilisation of linear peptides with biological activity. Molecules. 2020;25:3576 https://doi.org/10.3390/molecules25163576
7. Whiting M, Muldoon J, Lin YC, Silverman SM, Lindstron W, Olson AJ, et al. Inhibitors of HIV-1 protease by using in situ click chemistry. Angew Chem. 2006;118:1463–7. https://doi.org/10.1002/ange.200502161
8. Sampat S, Vadivelu M, Ravindran R, Perumal PT, Velkannan V, Karthikeyan K. Synthesis of 1,2,3-triazole tethered 3-hydroxy-2-oxindoles: promising corrosion inhibitors for steel in acidic medium and their anti-microbial evaluation. ChemistrySelect. 2020;5:2130–4. https://doi.org/10.1002/slct.201904320
9. Deswal S, Naveen, Tittal RK, Ghule VD, Lal K, Kumar A. 5-Fluoro-1H-indole-2,3-dione-triazoles- synthesis, biological activity, molecular docking, and DFT study. J Mol Struct. 2020;1209:127982 https://doi.org/10.1016/j.molstruc.2020.127982
10. Mazzotta S, Cebrero-Cangueiro T, Frattaruolo L, Vega-Holm M, CarreteroLedesma M, Sánchez-Céspedes J, et al. Exploration of piperazine-derived thioureas as antibacterial and anti-inflammatory agents. In vitro evaluation against clinical isolates of colistin-resistant Acinetobacter baumannii. Bioorg Med Chem Lett. 2020;30:127411 https://doi.org/10.1016/j.bmcl.2020.127411
11. Poonia N, Lal K, Kumar A. Design, synthesis, antimicrobial evaluation and in silico studies of symmetrical bis (urea-1,2,3-triazole) hybrids. Res Chem Intermed. 2021;47:1087–10103. https://doi.org/10.1007/s11164-020-04318-1
12. Moussaoui O, Bhadane R, Sghyar R, Ilas J, Hadrami EME, Chakroune S et al. Design, synthesis, in vitro and in silico characterization of new 2-quinolone-L-alaninate-1, 2, 3-triazoles as novel antimicrobial agents. ChemMedChem. 2022;17:e202100714 https://doi.org/10.1002/cmdc.202100714
13. Shafie A, Mohammadi-Khanaposhtani M, Asadi M, Rahimi N, Ranjbar PR, Ghasemi JB, et al. Novel fused 1, 2, 3-triazolo-benzodiazepine derivatives as potent anticonvulsant agents: design, synthesis, in vivo, and in silico evaluations. Mol Divers. 2020;24:179–89. https://doi.org/10.1007/s11030-019-09940-9
14. Patil PS, Kasare SL, Haval NB, Khedkar VM, Dixit PP, Rekha EM, et al. Novel isoniazid embedded triazole derivatives: synthesis, antitubercular and antimicrobial activity evaluation. Bioorg Med Chem Lett. 2020;30:127434 https://doi.org/10.1016/j.bmcl.2020.127434
15. Garg A, Borah D, Trivedi P, Gogoi D, Chaliha AK, Ali AA, et al. A simple work-up-free, solvent-free approach to novel amino acid linked 1,4-disubstituted 1,2,3-triazoles as potent antituberculosis agents. ACS Omega. 2020;5:29830–29837. https://doi.org/10.1021/acsomega.0c03862
16. Girase PS, Dhawan S, Kumar V, Shinde SR, Palkar MB, Karpoormath R. An appraisal of anti-mycobacterial activity with structure-activity relationship of piperazine and its analogues: a review. Eur J Med Chem. 2021;210:112967 https://doi.org/10.1016/j.ejmech.2020.112967
17. Deswal L, Verma V, Kumar D, Kaushik CP, Kumar A, Deswal Y, et al. Synthesis and antidiabetic evaluation of benzimidazole-tethered 1, 2, 3-triazoles. Arch Pharm. 2020;2020:e2000090 https://doi.org/10.1002/ardp.202000090

18. Theeramunkong S, Thiengsusuk A, Vajragupta O, Muhamad P. Synthesis, characterization and antimalarial activity of isoquinoline derivatives. Med Chem Res 2021;30:109–19. https://doi.org/10.1007/s00044-020-02642-0
19. Kaushik CP, Chahal M. Synthesis, antimalarial and antioxidant activity of coumarin appended 1, 4-disubstituted 1, 2, 3-triazoles. Monatsh Chem. 2021;152:1001–12. https://doi.org/10.1007/s00706-021-02821-8
20. Kandula MKR, Gundluru M, Nemallapudi BR, Gundala S, Kotha P, Zyryanov GV, et al. Synthesis, antioxidant activity, and α-glucosidase enzyme inhibition of α-aminophosphonate derivatives bearing piperazine-1,2,3-triazole moiety. J Heterocycl Chem. 2021;58:172–81. https://doi.org/10.1002/jhet.4157
21. Reddivari CKR, Devineni SR, Nemallapudi BR, Sravya G, Avula B, Shaik N, et al. Design, synthesis, biological evaluation and molecular docking studies of 1,4-disubstituted 1,2,3-triazoles: peg-400:h2o mediated click reaction of fluorescent organic probes under ultrasonic irradiation. Polycycl Aromat Compd. 2021. https://doi.org/10.1080/10406638.2021.1878246
22. Nural Y, Ozdemir S, Yalcin MS, Demir B, Atabey H, Seferoglu Z, et al. New bis-and tetrakis-1, 2, 3-triazole derivatives: synthesis, DNA cleavage, molecular docking, antimicrobial, antioxidant activity and acid dissociation constants. Bioorg Med Chem Lett. 2022;55:128453 https://doi.org/10.1016/j.bmcl.2021.128453
23. Shinoda K, Kanai M, Sohma Y. Design, synthesis, and properties of a chemically-tethered amyloid-# segment trimer resistant to inter-trimer mis-aggregation. J Org Chem. 2020;85:1635–43. https://doi.org/10.1021/acs.joc.9b02612
24. Kaushik CP, Sangwan J, Luxmi R, Kumar D, Kumar D, Das A, et al. Design, synthesis, anticancer and antioxidant activities of amide linked 1,4-disubstituted 1,2,3-triazoles. J Mol Struct. 2021;1226:129255 https://doi.org/10.1016/j.molstruc.2020.129255
25. Suryanarayana K, Robert AR, Kerru N, Pooventhiran T, Thomas R, Maddila S, et al. Design, synthesis, anticancer activity and molecular docking analysis of novel dinitrophenylpyrazole bearing 1, 2, 3-triazoles. J Mol Struct. 2021;1243:130865 https://doi.org/10.1016/j.molstruc.2021.130865
26. Begam R, Shajahan A, Vadivelu M. Synthesis of novel naphthalimide tethered 1, 2, 3-triazoles: in vitro biological evaluation and docking study of anti-inflammatory inhibitors. J Mol Struct. 2022;1254:132364 https://doi.org/10.1016/j.molstruc.2022.132364
27. Pertino MW, Torre AFDL, Hirschmann GS, Vega C, Rolon M, Coronel C, et al. Synthesis, trypanocidal and anti-leishmania activity of new triazole-lapachol and nor-lapachol hybrids. Bioorg Chem. 2020;103:104122 https://doi.org/10.1016/j.bioorg.2020.104122
28. El-Sayed WA, Khalaf HS, Mohamed SF, Hussien HA, Kutkat OM, Amr AE. Synthesis and antiviral activity of 1, 2, 3-triazole glycosides based substituted pyridine via click cycloaddition. Russ J Gen Chem. 2017;87:2444–53. https://doi.org/10.1134/S1070363217100279
29. Kumar H, Devaraji V, Joshi R, Jadhao M, Ahirkar P, Prasath R, et al. Antihypertensive activity of a quinoline appended chalcone derivative and its site specific binding interaction with a relevant target carrier protein. RSC Adv. 2015;5:65496–513. https://doi.org/10.1039/C5RA08778C
30. Cherif M, Horchani M, Ghamdi YOA, Almalki SG, Alqurashi YE, Jannet HB, et al. New pyrano-1,2,3-triazolopyrimidinone derivatives as anticholinesterase and antibacterial agents: Design, microwave-assisted synthesis and molecular docking study. J Mol Struct. 2020;1220:128685 https://doi.org/10.1016/j.molstruc.2020.128685
31. Igual MO, Nunes PSG, Costa RMD, Mantoani SP, Tostes RC, Carvalho I.Novel glucopyranoside C2-derived 1,2,3-triazoles displaying selective inhibition of O-GlcNAcase (OGA).Carbohydr Res.2019;471:43–55. https://doi.org/10.1016/j.carres.2018.10.007
32. Saghanezhad SJ, Buhamidi MM, Ebadi S, Taheri N, Sayyahi S. Entangled nanofbrous copper: an effcient and high performance nanostructured catalyst in azide-alkyne cycloaddition reaction and reduction of nitroarenes and aromatic aldehydes. React Kinet Mech Catal. 2021;133:897–911. https://doi.org/10.1007/s11144-021-02011-x
33. Barman K, Dutta P, Chowdhury D, Baruah PK. Green biosynthesis of copper oxide nanoparticles using waste colocasia esculenta leaves extract and their application as recyclable catalyst towards the synthesis of 1,2,3-triazoles. Bionanoscience. 2021;11:189–99. https://doi.org/10.1007/s12668-021-00826-5
34. Huisgen R, Szeimies G, Mobius L. 1.3-Dipolare cycloadditionen, XXXII. Kinetik der additionen organischer azide an CC-mehrfachbindungen. Chem Ber. 1967;100:2494–507. https://doi.org/10.1002/cber.19671000806
35. Tornøe CW, Christensen C, Meldal M. Peptidotriazoles on solid phase: [1,2,3]-triazoles by regiospecific copper(I)-catalyzed 1,3-dipolar cycloadditions of terminal alkynes to azides. J Org Chem. 2002;67:3057–64. https://doi.org/10.1021/jo011148j
36. Rostovtsev VV, Green LG, Fokin VV, Sharpless KB. A stepwise Huisgen cycloaddition process: copper(I)-catalyzed regioselective “ligation” of azides and terminal alkynes. Angew Chem Int Ed. 2002;41:2596–9. https://doi.org/10.1002/1521-3773(20020715)41:14%3C2596::aid-anie2596%3E3.0.co;2-4
37. Kaushik CP, Luxmi R. Synthesis and antimicrobial activity of 2-(4-(Hydroxyalkyl)-1H-1,2,3- triazol-1-yl)-N-substituted propanamides. J Heterocycl Chem. 2017;54:3618 https://doi.org/10.1002/jhet.2988
38. Chavan PV, Pandit KS, Desai UV, Kulkarni MA, Wadgaonkar PP. Cellulose supported cuprous iodide nanoparticles (Cell-CuI NPs): a new heterogeneous and recyclable catalyst for the one pot synthesis of 1,4-disubstituted – 1,2,3-triazoles in water. RSC Adv. 2014;4:42137–46. https://doi.org/10.1039/C4RA05080K
39. Kaushik CP, Chahal M. Synthesis and antibacterial activity of benzothiazole and benzoxazole-appended substituted 1,2,3-triazoles. J Chem Sci. 2020;132:142 https://doi.org/10.1007/s12039-020-01844-8
40. Kaushik CP, Luxmi R, Singh D, Kumar A. Synthesis and antimicrobial evaluation of ester-linked 1,4-disubstituted 1,2,3-triazoles with a furyl/thienyl moiety. Mol Divers. 2017;21:137–45. https://doi.org/10.1007/s11030-016-9710-y
41. Kaushik CP, Sangwan J, Luxmi R, Kumar D, Kumar D, Das A, et al. Design, synthesis, anticancer and antioxidant activities of amide linked 1,4-disubstituted 1,2,3-triazoles. J Mol Struct. 2021;1226:129255 https://doi.org/10.1016/j.molstruc.2020.129255
42. Lal K, Poonia N, Rani P, Kumar A, Kumar A. Design, synthesis, antimicrobial evaluation and docking studies of urea-triazole-amide hybrids. J Mol Struct. 2020;1215:128234 https://doi.org/10.1016/j.molstruc.2020.128234
43. MarvinSketch 19.19.0, 2019, ChemAxon (http://www.chemaxon.com)
44. Trott O, Olson AJ. J Comput Chem. 2010;31:455–61.
45. Dassault Systemes BIOVIA, Discovery studio visualizer v17.2.0.16349, San Diego: Dassault Systèmes, 2016.
46. Pettersen EF, Goddard TD, Huang CC, Couch GS, Greenblatt DM, Meng EC, et al. J Comput Chem. 2004;25:1605–12.
47. Sharma MK, Parashar S, Chahal M, Lal K, Pandya NU, Om H. Antimicrobial and in-silico evaluation of novel chalcone and amide-linked 1,4-disubstituted 1,2,3 triazoles. J Mol Struct. 2020;1257:132632 https://doi.org/10.1016/j.molstruc.2022.132632

Publisher’s note Springer Nature remains neutral with regard to jurisdictional claims in published maps and institutional affiliations.